

An Antibody-Catalyzed Isomerization Reaction

Tetsuo Uno, Jung Ku, James R. Prudent, Anita Huang, and Peter G. Schultz*

Contribution from the Howard Hughes Medical Institute, Department of Chemistry, University of California, Berkeley, California 94720

Received December 19, 1995[®]

Abstract: Monoclonal antibodies (mAbs) were generated against the coplanar transition state (TS[‡]) analogue **1** and assayed for their ability to catalyze the isomerization of bridged biphenyls **4**, **6**, and **7**. This is a relatively simple unimolecular reaction whose activation barrier arises from unfavorable steric interactions between the two benzylic methylene groups and strain in the bridging ring system. Seven mAbs were found that catalyzed the isomerization of **4** to **6**; the most efficient (mAb 64D8E10) has k_{cat} and K_{M} values of $4.3 \times 10^{-5} \text{ s}^{-1}$ and $420 \mu\text{M}$, respectively. This corresponds to a rate enhancement over the unimolecular uncatalyzed reaction ($k_{\text{cat}}/k_{\text{uncat}}$) of 2900. The dissociation constant for the TS[‡] analogue, K_{d} , was determined to be 210 nM. For both the antibody (64D8E10) catalyzed and uncatalyzed reactions, the free energy of activation (ΔG^{\ddagger}) is comprised largely of the enthalpy term; the antibody decreases the enthalpy of activation by 5 kcal/mol. Despite relatively large differences in the values of $k_{\text{cat}}/k_{\text{uncat}}$ for the five antibodies, the ratios of K_{d} to $K_{\text{M}}(\mathbf{4})$ are very similar. It is likely that the antibodies catalyze this reaction by reducing both ring strain and nonbonded steric interactions in the transition state.

Introduction

A number of strategies have been developed to generate catalytic antibodies, including the use of the transition state (TS[‡]) analogues to generate antibodies that stabilize a rate-determining transition state,¹ the use of antibody–hapten charge complementarity² or covalent antigenicity³ to elicit catalytic groups in antibody combining sites, and the use of antibodies as “entropy traps” to bring substrates together in a reactive configuration.⁴ Among these approaches, the use of transition state analogues has received the most attention.⁵ In order to directly assess the role of such analogues in eliciting catalytic antibodies, a relatively simple unimolecular reaction involving a single transition state is desirable.⁶ To this end, we have chosen to study the isomerization reaction of bridged biphenyls catalyzed by antibodies generated against the coplanar transition state analogue **1** (Figure 1).

The isomerization of bridged biphenyls has been extensively studied by Mislow and co-workers.^{7,8} This reaction involves

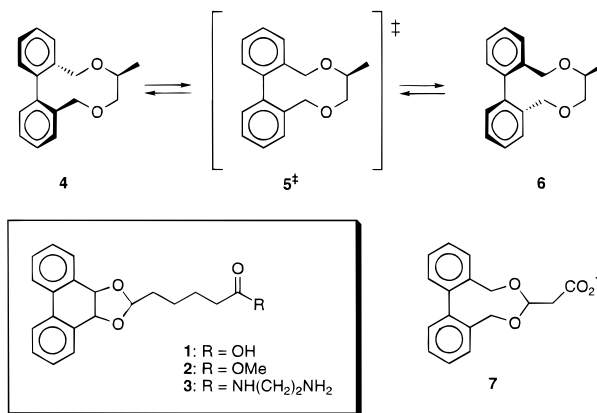


Figure 1. Antibody-catalyzed isomerization reaction and TS[‡] analogues.

rotation around a carbon–carbon σ bond, which in many cases proceeds slowly at room temperature due to nonbonded interactions between the benzylic protons and ring strain in the planar transition state. Typical activation energies are reported to be in the range of 20–26 kcal/mol and depend on ring size and substituents on the ring.^{7,8} This simple isomerization reaction is not likely to be catalyzed by general acids or bases, nucleophiles, or electrophiles. Rather a macromolecule that preferentially binds the planar transition state relative to the nonplanar substrate should, according to the classic notions of enzymatic catalysis of Pauling and Haldane,⁹ act as a catalyst. Our earlier work demonstrated that RNAs which selectively bind TS[‡] analogue **1** do indeed catalyze the isomerization reaction of bridged biphenyl **4** to its diastereomer **6**.¹⁰ Now we report that antibodies generated against hapten **1** can catalyze this isomerization reaction with significantly higher efficiency than that of the RNA molecule. Five different catalytic antibodies have been characterized with respect to their kinetic constants and affinities for transition state analogue **3**. The activation parameters, ΔH^{\ddagger} and ΔS^{\ddagger} , for both antibody-catalyzed and uncatalyzed reactions were also determined.

(9) (a) Pauling, L. *Chem. Eng. News* **1946**, *24*, 1375. (b) Haldane, J. B. S. *Enzymes*; Longmans Green: London, 1930.

(10) Prudent, J. R.; Uno, T.; Schultz, P. G. *Science* **1994**, *264*, 1924.

* To whom correspondence should be addressed.

[®] Abstract published in *Advance ACS Abstracts*, April 1, 1996.

(1) (a) Jacobs, J. W.; Schultz, P. G.; Sugawara, R.; Powell, M. J. *Am. Chem. Soc.* **1988**, *110*, 2174–2176. (b) Cochran, A. G.; Schultz, P. G. *Science* **1990**, *249*, 781.

(2) (a) Schokat, K. M.; Leumann, C.; Sugawara, R.; Schultz, P. G. *Nature* **1989**, *338*, 269–271. (b) Janda, K. D.; Weinhouse, M.; Schloeder, D. M.; Lerner, R. A.; Benkovic, S. J. *J. Am. Chem. Soc.* **1990**, *112*, 1274–1275. (c) Shokat, K.; Uno, T.; Schultz, P. G. *J. Am. Chem. Soc.* **1994**, *116*, 2261–2270.

(3) Wagner, J.; Lerner, R. A.; Barbas, C. F. *Science* **1995**, *270*, 1797.

(4) (a) Hilvert, D.; Hill, K. W.; Nared, K. D.; Auditor, M. J. *Am. Chem. Soc.* **1989**, *111*, 9261. (b) Braisted, A. C.; Schultz, P. G. *J. Am. Chem. Soc.* **1990**, *112*, 7430. (c) Braisted, A. C.; Schultz, P. G. *J. Am. Chem. Soc.* **1994**, *116*, 2211.

(5) (a) Lerner, R. A.; Benkovic, S. J.; Schultz, P. G. *Science* **1991**, *252*, 659–667. (b) Schultz, P. G.; Lerner, R. A. *Acc. Chem. Res.* **1993**, *26*, 391. (c) Schultz, P. G.; Lerner, R. A. *Science* **1995**, *269*, 1835–1842.

(6) Stewart, J. D.; Benkovic, S. J. *Nature* **1995**, *375*, 388–391.

(7) (a) Mislow, K.; Hyden, S.; Schaefer, H. J. *Am. Chem. Soc.* **1962**, *84*, 1449–1455. (b) Mislow, K.; Glass, M. A. W.; Hopps, H. B.; Simon, E.; Wahl, G. H. J. *J. Am. Chem. Soc.* **1964**, *86*, 1710–1733.

(8) (a) Mislow, K.; Glass, M. A. W.; O'Brien, R. E.; Rutkin, P.; Steinberg, D. H.; Weiss, J.; Djerassi, C. *J. Am. Chem. Soc.* **1964**, *86*, 1455–1478. (b) Mislow, K.; Hopps, H. B. *J. Am. Chem. Soc.* **1968**, *90*, 3018–3020. (c) Mislow, K.; Graeve, R.; Gordon, A. J.; Wahl, G. H. J. *J. Am. Chem. Soc.* **1973**, *95*, 1733–1741.

Experimental Section

General Methods. Unless otherwise noted, materials were obtained from commercial suppliers and used without further purification. Pyridine and CH_2Cl_2 were distilled under N_2 from CaH_2 immediately prior to use. THF was distilled under N_2 from Na/benzophenone immediately prior to use. All aqueous solutions were prepared from distilled H_2O which was further purified on a Milli-Q purification system. All moisture sensitive reactions were carried out in oven-dried glassware under a positive pressure of dry nitrogen. Analytical thin layer chromatography was performed on 0.25 mm precoated silica gel plates (Merck Fertigplatten, 60F-254, Art. 5765); compounds were visualized by UV light or by staining with iodine, ninhydrin, or phosphomolybdate. Flash silica gel chromatography was performed on Merck Kieselgel 60, 230–400 mesh.

Melting points were determined on a Meltemp device and are uncorrected. IR spectra were recorded on a Mattson Polaris Fourier transform spectrophotometer as thin films on NaCl plates or KBr pellets. Optical rotations were determined at 589 nm (sodium D line) with a Perkin-Elmer Model 241 polarimeter and a 10 cm path length cell. Rotations are reported as standard degree values ($[\alpha]_D = ^\circ\text{obs}[\text{path length (dm)}][\text{concentration (g/mL)}]$). UV spectra were recorded in 10 mm quartz cells on a Kontron Uvikon 860 spectrophotometer equipped with a constant temperature cell holder. ^1H resonances are reported in units of parts per million downfield from tetramethylsilane (TMS). Coupling constants (J) are given in hertz. All ^{13}C spectra were proton-decoupled, and ^{13}C resonances are reported in units of parts per million downfield from TMS.

Methyl 5-(Chlorocarbonyl)pentanoate (8). To adipic acid monomethyl ester (25.0 g, 0.156 mol) in 50 mL of benzene was added oxalyl chloride (25.0 g, 0.197 mol) over 3 min at 25 °C. The reaction was stirred at the same temperature for 30 min and then heated at reflux for another 30 min, after which time no starting acid was detected by IR. Benzene was removed by evaporation on a rotary evaporator. The resulting red residue was purified by distillation under reduced pressure, affording 25.2 g (91%) of a colorless oil: bp 51.5–52.0 °C (0.25 Torr); IR (film) 2955, 2872, 1801, 1740, 1438, 1205 cm^{-1} ; ^1H NMR (400 MHz, CDCl_3) δ 1.56 (m, 4H), 2.19 (t, 2H, $J = 6.8$), 2.79 (t, 2H, $J = 6.8$), 3.51 (s, 3H); ^{13}C NMR (100.6 MHz, CDCl_3) δ 23.3, 24.1, 32.9, 46.3, 51.2, 172.9, 173.0. Anal. Calcd for $\text{C}_7\text{H}_{11}\text{ClO}_3$: C, 47.07; H, 6.21; Cl, 19.85. Found: C, 47.50; H, 6.38; Cl, 19.48.

Methyl 5-Formylpentanoate (9). This procedure was adapted from that of Burgstahler *et al.*¹¹ In a 1 L round bottom flask were placed 500 mL of THF, 10% palladium on activated carbon (0.893 g), and 2,6-lutidine (5.82 mL, 50.0 mmol) under N_2 , and the flask was charged with H_2 . To the reaction was added acid chloride **8** (8.93 g, 50.0 mmol) dropwise over 3 min, and hydrogenation was performed using a H_2 balloon at 25 °C for 14 h with vigorous agitation. The catalyst and white precipitate formed during the reaction were filtered off using a Celite pad on filter paper, and the filtrate was concentrated *in vacuo*. The residue was taken up in 100 mL of ether, washed with 50 mL of 1 M HCl, saturated aqueous sodium bicarbonate, and saturated aqueous NaCl, dried over anhydrous magnesium sulfate, filtered, and concentrated *in vacuo*. The resulting colorless residue was purified by distillation under reduced pressure, affording 3.86 g (53%) of a colorless oil: bp 54.0–54.5 °C (0.45 Torr); IR (film) 2945, 2745, 1732, 1191, 1164 cm^{-1} ; ^1H NMR (400 MHz, CDCl_3) δ 1.63 (m, 4H), 2.31 (m, 2H), 2.43 (m, 2H), 3.64 (s, 3H), 9.73 (d, 1H, $J = 1.3$); ^{13}C NMR (100.6 MHz, CDCl_3) δ 21.2, 24.1, 33.3, 43.1, 51.1, 173.2, 201.7. Anal. Calcd for $\text{C}_7\text{H}_{12}\text{O}_3$: C, 58.32; H, 8.39. Found: C, 58.43; H, 8.56.

cis-O,O'-(5-(Methoxycarbonyl)pentylidene)-9,10-dihydrophenanthrene-9,10-diol (2). A mixture of *cis*-9,10-dihydrophenanthrene-9,10-diol¹² (68 mg, 320 μmol), aldehyde **9** (55 mg, 380 μmol), and *p*-toluenesulfonic acid monohydrate (6.1 mg, 32 μmol) in 3 mL of THF was stirred at 25 °C for 20 h. Ten milliliters of chloroform was added, and the reaction mixture was washed with 1 mL of saturated aqueous sodium bicarbonate. The organic layer was separated, dried over anhydrous sodium sulfate, filtered, and concentrated *in vacuo*. The

residue was purified by flash chromatography on a 2×18 cm silica gel column (25% [v/v] ethyl acetate in hexanes; $R_f = 0.36$), affording 82 mg (76%) of a colorless oil: IR (film) 3064, 3015, 2936, 2864, 1735, 1460, 1427, 1220, 1127 cm^{-1} ; ^1H NMR (400 MHz, CDCl_3) δ 1.30 (m, 2H), 2.19 (t, 2H, $J = 7.6$), 3.63 (s, 3H), 5.15 (s, 2H), 5.28 (t, 1H, $J = 4.8$), 7.35 (dt, 2H, $J = 7.4, 0.9$), 7.42 (dt, 2H, $J = 7.6, 1.4$), 7.45 (dd, 2H, $J = 1.3, 7.5$), 7.89 (d, 2H, $J = 7.5$), 10.5 (br s, 1H); ^{13}C NMR (100.6 MHz, CDCl_3) δ 23.5, 24.7, 33.9, 34.2, 51.4, 74.5, 103.9, 123.3, 128.2, 129.2, 130.3, 131.4, 132.0, 174.0; mass spectrum (FAB^+) m/e 339.0 (MH^+), 345.0 (MLi^+); exact mass calcd for $\text{C}_{21}\text{H}_{22}\text{O}_4\text{Li}^+$ 345.1678, found 345.1671.

cis-O,O'-(5-Carboxypentylidene)-9,10-dihydrophenanthrene-9,10-diol (1). Ester **2** (34.7 mg, 103 μmol) was dissolved in 1 mL of ethanol, and 210 μL of 1 M aqueous NaOH was added. The reaction was stirred at 25 °C for 24 h, after which time TLC analysis (25% [v/v] ethyl acetate in hexanes) showed no starting material. Ethanol was removed by concentration *in vacuo*. The residue was taken up in 1.5 mL of CHCl_3 and washed with 1.5 mL of 1 M HCl. The organic layer was separated, dried over anhydrous sodium sulfate, filtered, and concentrated *in vacuo*, affording 29 mg (87%) of a white solid: mp 135–137 °C; IR (KBr) 3046 (br), 2923, 2885, 1700, 1453, 1423, 1300, 1246, 1200, 1138, 1000 cm^{-1} ; ^1H NMR (400 MHz, CDCl_3) δ 1.30 (m, 2H), 1.45 (m, 4H), 2.19 (t, 2H, $J = 5.0$), 5.13 (s, 2H), 5.27 (t, 1H, $J = 4.7$), 7.32 (dt, 2H, $J = 1.1, 7.4$), 7.40 (dt, 2H, $J = 1.4, 7.6$), 7.53 (dd, 2H, $J = 1.4, 7.5$), 7.87 (d, 2H, $J = 7.8$); ^{13}C NMR (100.6 MHz, CDCl_3) δ 23.4, 24.4, 33.8, 34.2, 74.6, 103.9, 123.3, 128.2, 129.2, 130.3, 131.5, 132.0, 179.4; mass spectrum (FAB^+) m/e 324 (M^+); exact mass calcd for $\text{C}_{20}\text{H}_{20}\text{O}_4$ 324.1361, found 324.1352.

cis-O,O'-(5-[N-(2-Aminoethyl)carbamoyl]pentylidene)-9,10-dihydrophenanthrene-9,10-diol (3). Compound **1** (500 mg, 1.54 mmol) was added to ethylenediamine (0.93 g, 1.54 mmol), *N*-hydroxysuccinimide (0.177 g, 1.54 mmol), and 1,3-dicyclohexylcarbodiimide (0.317 g, 1.54 mmol) in 50 mL of chloroform and stirred at 25 °C for 1 h. The precipitate was filtered off, and the reaction was washed twice with 50 mL of water and once with 50 mL of saturated aqueous sodium bicarbonate, dried over anhydrous sodium sulfate, filtered, and concentrated *in vacuo* to afford 338 mg (60%) of an off-white solid: mp 99–103 °C; IR (KBr) 3323 (br), 3069, 2946, 2923, 2869, 1650, 1539, 1450, 1125, 1070 cm^{-1} ; ^1H NMR (400 MHz, CDCl_3) δ 1.27 (m, 2H), 1.45 (m, 2H), 1.52 (m, 2H), 2.03 (t, 2H, $J = 7.6$), 2.75 (t, 2H, $J = 5.8$), 3.22 (q, 2H, $J = 5.8$), 3.50 (br s, 2H), 5.13 (s, 2H), 5.26 (t, 1H, $J = 4.8$), 5.83 (br s, 1H), 7.36 (t, 2H, $J = 7.4$), 7.34 (t, 2H, $J = 6.9$), 7.53 (d, 2H, $J = 6.1$), 7.87 (d, 2H, $J = 7.2$); ^{13}C NMR (100.6 MHz, CDCl_3) δ 23.5, 25.4, 34.1, 36.4, 41.1, 41.4, 74.4, 103.9, 123.2, 128.2, 129.1, 130.3, 131.3, 131.9, 173.4; mass spectrum (FAB^+) m/e 367 (MH^+); exact mass calcd for $\text{C}_{22}\text{H}_{27}\text{N}_2\text{O}_3$ 367.2021, found 367.2017.

2(S)-Methyl-(S or R)-dibenzof[*f,h*]-1,4-dioxacyclodeca-6,8-diene (4 and 6). Sodium hydride (1.60 g, 60% in oil, 40.0 mmol) was placed in a 500 mL flask equipped with a condenser, washed three times with 20 mL of petroleum ether, and suspended in 300 mL of THF. (S)-1,2-Propanediol (732 μL , 10.0 mmol) was added, and the reaction was heated at reflux for 2 h. A solution of 2,2'-bis(bromomethyl)biphenyl (3.40 g, 10.0 mmol) in 50 mL of THF was added in one portion, and the reaction was heated at reflux for an additional 16 h. The remaining sodium hydride was destroyed by addition of water, and the reaction mixture was concentrated *in vacuo*. The residue was taken up in 50 mL of water and extracted three times with 50 mL of ether. The combined organic layers were washed with 100 mL of saturated aqueous NaCl, dried over anhydrous magnesium sulfate, filtered, and concentrated *in vacuo*. The residue was distilled using a Buchi GKR-51 apparatus to remove high boiling point byproducts. Two diastereomeric products were isolated from the distillate by flash chromatography on a 2.5×25 cm silica gel column (9% [v/v] ethyl acetate in hexanes; $R_f(\mathbf{4}) = 0.23$; $R_f(\mathbf{6}) = 0.18$), affording colorless solids, 282 mg (11%) for **4** and 256 mg (10%) for **6**. Each isomer was further purified by recrystallization from petroleum ether to yield colorless needles. Data for **4**: mp 112–114 °C; IR (KBr) 3015, 2986, 2967, 2917, 2653, 1077 cm^{-1} ; ^1H NMR (250 MHz, CDCl_3) δ 1.10 (d, 3H, $J = 6.5$), 3.23 (dd, 1H, $J = 12.9, 7.0$), 3.56 (ddq, 1H, $J = 2.2, 7.0, 6.5$), 3.70 (dd, 1H, $J = 2.2, 12.9$), 4.44 (d, 1H, $J = 10.1$), 4.52 (d, 1H, $J = 11.1$), 4.54 (d, 1H, $J = 10.1$), 4.80 (d, 1H, $J = 11.1$), 7.12 (d, 2H, $J = 7.3$), 7.36 (m, 4H), 7.36 (m, 2H); ^{13}C NMR (100.6 MHz, CDCl_3) δ 17.9, 69.6, 70.6,

(11) Burgstahler, A. W.; Weigel, L. O.; Shaefer, L. G. *Synthesis* **1976**, 767–768.

(12) Criegee, R.; Marchand, B.; Wannowius, H. *Ann. Chem.* **1942**, 550, 99.

71.4, 75.8, 127.8, 127.9, 128.0, 128.0, 129.7, 130.4, 130.8, 131.0, 136.6, 137.0, 140.4, 140.8; mass spectrum (FAB⁺) *m/e* 255.2 (MH⁺). Anal. Calcd for C₁₇H₁₈O₂: C, 80.28; H, 7.13. Found: C, 80.02; H, 7.25. Data for **6**: mp 101–102 °C; IR (KBr) 3062, 3018, 2969, 2933, 2879, 1084 cm⁻¹; ¹H NMR (250 MHz, CDCl₃) δ 0.94 (d, 3H, *J* = 6.5), 3.26 (dd, 1H, *J* = 12.2, 8.9), 3.38 (dd, 1H, *J* = 2.4, 12.2), 3.62 (ddq, 1H, *J* = 2.9, 8.9, 6.5), 4.22 (d, 1H, *J* = 11.9), 4.28 (d, 1H, *J* = 12.8), 4.64 (d, 1H, *J* = 11.8), 4.91 (d, 1H, *J* = 12.7), 7.14 (m, 2H), 7.33 (m, 6H); ¹³C NMR (100.6 MHz, CDCl₃) δ 16.8, 69.1, 70.0, 70.2, 73.0, 127.3, 127.8, 127.8, 128.2, 129.2, 129.3, 129.3, 129.8, 136.1, 137.0, 142.0, 142.1; mass spectrum (FAB⁺) *m/e* 255.2 (MH⁺). Anal. Calcd for C₁₇H₁₈O₂: C, 80.28; H, 7.13. Found: C, 80.16; H, 7.28.

2-[(Methoxycarbonyl)methyl]dibenzo[*e,g*]-1,3-dioxacyclonona-5,7-diene (11). 2,2'-Biphenyldimethanol (2.14 g, 10.0 mmol) and methyl 3,3-dimethoxypropionate (1.42 mL, 10.0 mmol) were dissolved in 150 mL of benzene and heated at reflux for 3 h in the presence of concentrated sulfuric acid (2 drops). The reaction solution was concentrated on a rotary evaporator to about 1/3 volume, washed with 50 mL each of 10% aqueous sodium bicarbonate and saturated aqueous NaCl, dried over anhydrous sodium sulfate, filtered, and concentrated *in vacuo*. The residue was purified by flash chromatography on a 4 × 18 cm silica gel column (9% [v/v] ethyl acetate in hexanes; *R*_f = 0.26), affording 1.55 g (52%) of a colorless oil which solidified after sitting at 25 °C: mp 77–78 °C; IR (film) 3057, 3019, 2951, 1742, 1117, 1034 cm⁻¹; ¹H NMR (400 MHz, CDCl₃) δ 2.70 (d, 2H, *J* = 5.6), 3.68 (s, 3H), 4.06 (d, 1H, *J* = 12.4), 4.26 (d, 1H, *J* = 12.1), 4.51 (d, 1H, *J* = 12.1), 4.70 (d, 1H, *J* = 12.4), 4.77 (t, 1H, *J* = 5.6), 7.21 (d, 2H, *J* = 6.1), 7.39 (m, 4H), 7.46 (d, 1H, *J* = 7.3), 7.51 (d, 1H, *J* = 7.4); ¹³C NMR (100.6 MHz, CDCl₃) δ 41.3, 51.7, 65.4, 74.4, 101.3, 128.0, 128.5, 128.6, 128.6, 129.7, 129.9, 130.5, 130.6, 134.6, 136.4, 141.4, 142.0, 170.6; mass spectrum (FAB⁺) *m/e* 299 (MH⁺). Anal. Calcd for C₁₈H₁₈O₄: C, 72.47; H, 6.08. Found: C, 72.57; H, 6.12.

2-(Carboxymethyl)dibenzo[*e,g*]-1,3-dioxacyclonona-5,7-diene (7). Compound **11** (0.298 g, 1.00 mmol) was dissolved in 10 mL of ethanol, and 2 mL of 1 M aqueous NaOH was added. The reaction was stirred at 25 °C for 14 h, and concentrated *in vacuo*. The residue was taken up in 50 mL of ethyl acetate and washed with 10 mL of 1 N H₂SO₄ and 50 mL of saturated aqueous NaCl, dried over anhydrous sodium sulfate, filtered, and concentrated *in vacuo*, affording 0.272 g (96%) of a white solid: mp 140–142 °C; IR (KBr) 3062, 3015, 2939, 2892, 1700, 1439, 1307, 1246, 1200, 1108, 1023 cm⁻¹; ¹H NMR (400 MHz, CDCl₃) δ 2.73 (d, 2H, *J* = 5.4), 4.02 (d, 1H, *J* = 12.5), 4.26 (d, 1H, *J* = 12.1), 4.52 (d, 1H, *J* = 12.2), 4.71 (d, 1H, *J* = 12.4), 4.73 (t, 1H, *J* = 5.4), 7.21 (m, 2H), 7.39 (m, 6H), 10.9 (br s, 1H); ¹³C NMR (100.6 MHz, CDCl₃) δ 41.2, 65.4, 74.5, 100.9, 128.0, 128.5, 128.6, 128.7, 129.7, 129.9, 130.5, 134.4, 136.1, 141.3, 142.0, 175.6; mass spectrum (FAB⁺) *m/e* 285 (MH⁺). Anal. Calcd for C₁₇H₁₆O₄: C, 71.82; H, 5.67. Found: C, 71.96; H, 5.71.

Resolution of 7. A typical procedure is as follows. Racemic acid **7** (0.736 g, 2.59 mmol) was dissolved in a minimum amount of hot ethyl acetate. Brucine (0.561 g, 1.50 mmol) was added in one portion, and the reaction was allowed to cool slowly on the bench top. The precipitate formed was collected by vacuum filtration, and dried under reduced pressure, affording 0.934 g of a white solid. Optical purity was determined by HPLC analysis on a reversed-phase chiral HPLC column (Daicel, CHIRALCEL OD-R, 0.46 × 25 cm) using 40% acetonitrile in a 1 M sodium perchlorate buffer (pH 3.0) as eluent. The analysis of the precipitate indicated an 84.4% enantiomeric excess (ee). To liberate the free acid, the precipitate (0.93 g) was suspended in 10 mL of ethyl acetate, and washed with 10 mL of ice cold 1 N sulfuric acid, followed by 10 mL of saturated aqueous NaCl. The organic layer was dried over anhydrous sodium sulfate, filtered, and concentrated *in vacuo*, affording 0.374 g of a clear oil. Usually three rounds of the resolution operation were satisfactory for 99% ee optical enrichment: (+)-**7**; [α]_D = +7.5° (*c* 0.102, ethanol).

Bovine Serum Albumin (BSA) and Keyhole Limpet Hemocyanin (KLH) Conjugates of the Hapten. To a solution of **1** (20 mg, 62 μmol) and *N*-hydroxysuccinimide (7.1 mg, 62 μmol) in 1 mL of DMF was added dicyclohexylcarbodiimide (12.8 mg, 62 μmol), and the reaction was stirred at 25 °C for 5 h. BSA (20 mg, fraction V, Sigma) and KLH (20 mg, Sigma) were dissolved each in 4.5 mL of a 0.1 M borate buffer (pH 8.0). To each protein solution was added 0.5 mL of

the DMF solution. Both reaction mixtures became very cloudy. The addition of 1 mL of DMF made each reaction clear again. The reactions were stirred gently at 25 °C for 16 h, and the protein conjugates were exhaustively dialyzed against a phosphate-buffered saline (PBS; 10 mM sodium phosphate, 150 mM NaCl, pH 7.2). Any insoluble material after dialysis was removed by centrifugation at 14 000 rpm for 5 min followed by filtration through a 0.2 μm membrane filter unit. Protein concentrations of the final solutions were determined by the method of Bradford.¹³ The epitope densities (ratio of conjugated hapten molecules per carrier protein molecule) were determined to be 17 for the BSA conjugate and 66 for the KLH conjugate by comparing the absorbance at 270 nm between the hapten–protein conjugate and native protein of the same concentration, using ε₂₇₀ = 16 900 for the hapten.

Antibody Production and Purification. Monoclonal antibodies specific for hapten **1** were generated using standard hybridoma technology.¹⁴ BALB/c mice were immunized by intraperitoneal injection of 200 μL of an emulsion of the KLH conjugate (100 μg) in complete Freund's adjuvant. After 2 weeks the mice were immunized again with the KLH conjugate in incomplete Freund's adjuvant. After an additional 4 weeks, the mice were boosted intraperitoneally with the KLH conjugate in PBS. Fusions were performed 5 days later. Spleenocytes from two BALB/c mice were fused with 2 × 10⁸ myeloma cells (P3X63AG8.653)¹⁵ in a solution of 50% polyethylene glycol (Merck, GC grade PEG 4,000), plated into eighty 96-well plates and grown on AH media (azaserine- and hypoxanthin-supplemented DME media) for the hybridoma selection. Hybridomas were screened by enzyme-linked immunosorbent assay (ELISA) using the BSA conjugate. After cloning by the method of limited dilution, 37 lines of monoclonal hybridomas were isolated. Ascitic fluid was produced in pristane-primed BALB/c mice for each cell line.

Antibodies were purified by protein A affinity chromatography using a procedure adapted from that of Fagerstam *et al.*¹⁶ A 10 mL sample of ascitic fluid was diluted with 20 mL of binding buffer (aqueous 1.5 M glycine, 3.0 M NaCl, pH 8.9), and the solution was filtered through a 0.45 μm membrane filter. The filtrate was then loaded onto a 10 mL column of Affinica protein A-agarose (Schleicher and Schuell) preequilibrated with binding buffer. The column was washed with binding buffer until the absorbance of the eluent was less than 0.05 absorbance unit at 280 nm. Antibodies were eluted from the column by elution buffer (100 mM sodium citrate, pH 3.0), and 3.0 mL fractions were collected into tubes containing 1.0 mL of collecting buffer (1.0 M Tris, pH 9.0) for rapid neutralization. The fractions containing antibodies were combined and dialyzed exhaustively against PBS (10 mM sodium phosphate, 100 mM NaCl, 0.02% sodium azide, pH 7.0). Protein concentrations were determined by absorbance at 280 nm (1.37 absorbance units for 1.0 mg/mL immunoglobulin G and a molecular weight of 150 000). Antibodies were concentrated by a centiprep-30 apparatus (Amicon) if necessary. Antibodies were judged to be >95% pure by SDS–polyacrylamide gel with Coomassie blue staining.

Fab Preparation and Purification. This procedure is based on the instructions from the supplier of the immobilized papain gel. A solution of antibody 64D8E10 in a 20 mM phosphate, 10 mM EDTA buffer, pH 7.0, was concentrated by a centiprep-30 concentrator (Amicon) to 19.6 mg/mL. One milliliter of immobilized papain on agarose (Pierce, product number 20341) was suspended in 4 mL of freshly prepared digestion buffer (20 mM phosphate, 10 mM EDTA, 20 mM cysteine, pH 7.0) in a 15 mL polypropylene tube and centrifuged, and the supernatant was discarded. The operation was repeated again. To the papain gel was added 0.5 mL of antibody solution, and the reaction was vigorously shaken at 37 °C for 6 h. The reaction was quenched by adding 1.5 mL of a 10 mM Tris buffer (pH 7.5) and centrifuged. The supernatant was diluted with 2 volumes of protein A binding buffer and loaded onto 3 mL of protein A gel. The protein A column was washed with binding buffer, and fractions

(13) Bradford, M. M. *Anal. Biochem.* **1976**, *72*, 248–254.

(14) (a) Goding, J. *Monoclonal Antibodies: Principles and Practice*, 2nd ed.; Academic Press: New York, 1986. (b) Harlow, E.; Lane, D. *Antibodies. A Laboratory Manual*; Cold Spring Harbor Laboratory: New York, 1988.

(15) Kearney, J. F.; Radbruch, A.; Liesegang, B.; Rajewsky, K. *J. Immunol.* **1979**, *123*, 1548–1550.

(16) Fredriksson, U. B.; Fagerstam, L. G.; Cole, A. W. G.; Lundgren, T. *Protein A-Sepharose C1-4B Affinity Purification of IgG Monoclonal Antibodies*; Pharmacia AB: Uppsala, Sweden, 1986.

containing proteins were pooled and dialyzed exhaustively against a 10 mM MOPS (3-(*N*-morpholino)propanesulfonic acid), 150 mM NaCl buffer (pH 7.2). The resulting solution was concentrated using a centricon-10 concentrator (Amicon) to about 20 mg/mL and further purified by gel filtration chromatography. A 500 μ L sample of the solution was loaded onto a Superdex 75 HR 10/30 column (10 \times 300 mm, Pharmacia), and the Fab fragment was eluted with a 10 mM MOPS, 150 mM NaCl buffer (pH 7.2) at a constant flow rate of 1.0 mL/min. The fractions containing the pure Fab fragment were used for the BIAcore assay. The Fab fragments of the remaining antibodies (51F3D2, 56D10D6, 83F11C4, 83F12D6) were prepared in the same manner.

Antibody Kinetics and Product Analysis. Initial velocities were determined by reversed-phase HPLC analysis. The reaction was initiated by adding 196 μ L of antibody solution in a 10 mM MOPS, 10 mM NaCl buffer (pH 7.2) to 4 μ L of substrate (**4** or **6**) stock solution in DMSO. The reaction was incubated at 35 $^{\circ}$ C, and quenched by the addition of 200 μ L of CH₃CN prior to <1% substrate depletion. Precipitated proteins were removed by centrifugation, followed by filtration through a 0.45 μ m membrane filter. A 100 μ L aliquot of the filtrate was applied to reversed-phase HPLC (Microsorb 5 μ m C18, 4.6 mm \times 25 cm) which was then eluted with 80% CH₃CN in H₂O over 10 min. Peaks were monitored at 220 nm and quantified by comparing the relative peak area with a standard calibration curve. The retention times for **4** and **6** were 6.1 and 5.4 min, respectively. For kinetic analysis of the **4** to **6** isomerization, the following substrate concentrations were used: 100, 200, 300, 400, 500, and 600 μ M. The uncatalyzed rates were determined in the absence of the antibodies under otherwise identical conditions. The kinetic parameters V_{\max} and K_M were determined by plotting reaction rate v as a function of **[4]** and fitting the data to the Michaelis–Menten equation $v = V_{\max} [\mathbf{4}] / (K_M + [\mathbf{4}])$ using the Levenberg–Marquardt algorithm of the Kaleida Graph computer program (Abelbeck software). For assays using substrate (+)-**7**, a chiral reversed-phase HPLC column (Daicel, CHIRALCEL OD-R, 0.46 \times 25 cm) was used for HPLC analysis. Peaks were eluted with 40% CH₃CN in a 1 M aqueous NaClO₄ buffer, pH 3.0, over 25 min, and monitored at 220 nm. Retention times for the substrate and product were 21.7 and 19.9 min, respectively.

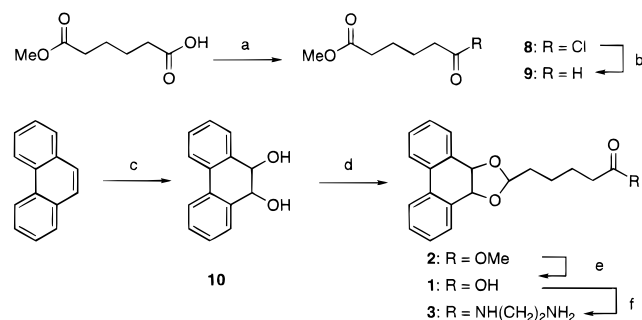
Surface Plasmon Resonance Assay (BIAcore Assay). The BIAcore assay was performed on a BIAcore 2000 instrument (Pharmacia). A 35 μ L sample of activation solution containing 200 mM *N*-ethyl-*N'*-[3-(dimethylamino)propyl]carbodiimide hydrochloride (EDC) and 50 mM *N*-hydroxysuccinimide (NHS) was injected over a CM-5 sensor chip surface at 5 μ L/min at 25 $^{\circ}$ C. A 15 μ L portion of hapten **3** solution (0.5 mM in a 10 mM MOPS, 10 mM NaCl, pH 7.2, buffer) was then injected at 5 μ L/min at 25 $^{\circ}$ C. The unreacted NHS esters on the surface were blocked with 35 μ L of 1.0 M ethanolamine. Fab fragments (200–900 nM, 80 μ L) in a 10 mM MOPS, 150 mM NaCl, pH 7.2, buffer were injected over the chip surface at 40 μ L/min. The signals were recorded and analyzed using programs provided by the manufacturer.

Results and Discussion

Hapten Design. The isomerization reaction of seven- to nine-membered ring bridged biphenyls is thought to involve transition states in which the two phenyl rings are coplanar.⁷ In the isomerization of a seven-membered ring bridged biphenyl, the activation barrier arises largely from ring strain. In contrast, for a nine-membered ring bridged biphenyl, the two benzylic carbons are only 1.4 \AA apart in the transition state, resulting in unfavorable nonbonded steric interactions; the transition state conformation of this ring system is almost without ring strain. Both ring strain and nonbonded interactions contribute to the activation barrier for the isomerization of an eight-membered ring bridged biphenyl.

In order to mimic the coplanar transition state for biphenyl isomerization, we chose a dihydrophenanthrene ring system with a fused five-membered acetal ring (Figure 1). For dihydrophenanthrene, Mislow estimated a dihedral angle of 15 $^{\circ}$ and an activation barrier of 4 kcal/mol for isomerization.⁷ Indeed, the ¹H NMR spectrum of hapten **1** shows only one sharp singlet

Scheme 1^a



^a (a) Oxalyl chloride, C₆H₆, 80 $^{\circ}$ C, 91%; (b) H₂, 2,6-lutidine, 10% Pd/C, THF, 25 $^{\circ}$ C, 50%; (c) OsO₄, pyridine, C₆H₆, 25 $^{\circ}$ C; mannitol, KOH, CH₂Cl₂/H₂O, 63%; (d) **9**, PTS, THF, 25 $^{\circ}$ C, 76%; (e) NaOH, H₂O/EtOH, 25 $^{\circ}$ C; H⁺, 87%; (f) ethylenediamine, NHS, DCC, CHCl₃, 25 $^{\circ}$ C, 60%.

for the benzylic protons, demonstrating rapid equilibration of the ring system. In order to mimic the bridge moiety, we introduced a cyclic *cis*-acetal into the dihydrophenanthrene hapten. The acetal moiety also serves as the linker to carrier proteins (small, nonpeptidyl molecules such as hapten **1** are not immunogenic unless they are first conjugated to a carrier protein). This linkage scheme should result in antibodies that bind tightly to the two coplanar phenyl rings, but which may bind with lower affinity to the bridging acetal due to its proximity to the carrier protein.

The isomerization reaction was assayed using two different substrates (Figure 1). The first has a 10-membered ring bridge containing an ethylenediol spacer to facilitate synthesis. In order to simplify substrate isolation and kinetic analysis by HPLC, a chiral center was also introduced into the 10-membered ring bridge to afford the diastereomeric substrate and product, **4** and **6**. The alternative substrate **7** was also prepared which has a nine-membered ring bridge without a chiral center, and therefore more closely resembles the structure of the hapten. Substrate **7** has a carboxylic acid group which provides a handle for optical resolution and improved solubility.

Earlier work demonstrated that an RNA molecule which binds the planar transition state analogue **1** can also catalyze the isomerization reaction of bridged biphenyl **4** to its diastereomer **6**.¹⁰ The RNA-catalyzed reaction was shown to follow classical Michaelis–Menten kinetics with a k_{cat} of $4.7 \times 10^{-7} \text{ s}^{-1}$ and a K_M of 540 μ M at 28 $^{\circ}$ C (corresponding to a $k_{\text{cat}}/k_{\text{uncat}}$ of 88). The RNA-catalyzed reaction was competitively inhibited by ligand **2** with a K_i of 7 μ M. We found a good correlation between $k_{\text{cat}}/k_{\text{uncat}}$ and K_M/K_i for the RNA-catalyzed reaction, which suggests that hapten **1** is acting as a good transition state mimic. Since the catalytic efficiency is correlated with preferential binding affinity for the transition state, higher catalytic rates may be achieved with antibodies whose affinities are, in general, significantly higher than those of RNA aptamers.¹⁷

Synthesis and Antibody Production. The synthesis of hapten **1** is illustrated in Scheme 1. The linker **9** was synthesized from adipic acid monomethyl ester by a modified Rosenmund reduction¹¹ of acid chloride **8**. Phenanthrene was treated with an equimolar amount of osmium tetroxide and 2 equiv of pyridine in benzene to yield the osmate ester which was then hydrolyzed to *cis*-diol **10** with a solution of mannitol and potassium hydroxide in dichloromethane/water.¹² Reaction of **9** and **10** in THF in the presence of *p*-toluenesulfonic acid as catalyst afforded the dihydrophenanthrenediol acetal. There are *cis* and *trans* isomers for this cyclic acetal, but only one was

(17) (a) Bartel, D. P.; Szostak, J. W. *Science* **1993**, *261*, 1411. (b) Green, R.; Szostak, J. W. *Science* **1992**, *258*, 1910.

obtained, presumably the *trans* form. The methyl ester moiety of **2** was hydrolyzed using sodium hydroxide or lithium hydroxide in ethanol/water to afford hapten **1** in the free acid form after acidic workup. The ethylenediamine monoamide of the hapten (**3**) was prepared by reaction of hapten **1** with 1 equiv of ethylenediamine using *N*-hydroxysuccinimide (NHS) and 1,3-dicyclohexylcarbodiimide (DCC). The UV spectrum of **1** revealed a characteristic biphenyl conjugation band at 270 nm, very similar to that of dihydrophenanthrene.⁷

The diastereomeric substrates **4** and **6** were prepared by condensation of the disodium (*S*)-1,2-propanedialkoxide salt and 2,2'-bis(bromomethyl)biphenyl in THF. The diastereomers **4** and **6** had significantly different polarities and were isolable by chromatography on silica gel. Upon recrystallization from petroleum ether, the pure diastereomers were obtained. The X-ray crystal structure of isomer **6** revealed that it had the (*R,S*) configuration, indicating that **4** has the (*S,S*) configuration.¹⁰ The crystal structure also revealed a dihedral angle of 68° between the two phenyl rings. Mislow also estimated a dihedral angle of 68° for a nine-membered ring bridged biphenyl.⁷ UV spectra of **4** or **6** showed no biphenyl conjugation band in the region of 250 nm, consistent with a large angle between two phenyl rings with no significant conjugation between them.⁷ ¹H NMR and HPLC analysis indicated that **4** and **6** interconvert slowly at room temperature.

Substrate **7** was synthesized in racemic form by an acetal exchange reaction of methyl 3,3-dimethoxypropionate with 2,2'-biphenyldimethanol, followed by base hydrolysis of the ester moiety. Resolution of the racemic acid was performed using brucine as the chiral base, affording optically enriched precipitate. Upon treatment with acid, the precipitate liberated (+)-**7**. After several rounds of recrystallization, optically active substrate (+)-**7** was obtained in 99% ee as determined by reversed-phase chiral HPLC analysis. The absolute configuration of (+)-**7** has yet to be determined.

For hybridoma production, hapten **1** was conjugated to keyhole limpet hemocyanin (KLH) and bovine serum albumin (BSA) via the activated *N*-hydroxysuccinimide ester to give epitope densities of 17 haptens per BSA molecule and 66 for KLH. Spleenocytes from two BALB/c mice immunized with the KLH conjugate were fused with myeloma cells (P3X63AG8.653),¹⁵ and the resulting hybridoma supernatants were screened by ELISA (enzyme-linked immunosorbent assay) for antibody binding to the BSA·hapten conjugate.¹⁴ Thirty-seven monoclonal cell lines were isolated after cloning by the limiting dilution method.¹⁴ Thirty-two antibodies specific to hapten **1** were obtained from ascitic fluid and purified by protein A affinity chromatography.¹⁶ Antibodies were determined to be >95% homogeneous by SDS–polyacrylamide gel electrophoresis with Coomassie blue staining.

Kinetics and Inhibition of Antibody Catalysis. Of the 32 monoclonal antibodies (mAbs) that were specific for hapten **1**, 7 catalyzed the isomerization of substrate **4** (*S,S*) to product **6** (*R,S*). These seven antibodies also catalyzed the reverse reaction of **6** to **4**, consistent with the notion of microscopic reversibility. Six of 32 antibodies catalyzed the racemization of substrate (+)-**7**. Interestingly, only one antibody, 51F3D2, catalyzed the isomerization of both substrates, but with moderate catalytic efficiency in each case. Antibody 64D8E10 had significantly higher catalytic activity for the isomerization of **4** to **6** than any other antibody, but catalyzed the racemization of (+)-**7** poorly. In contrast, antibody 50A3C12 did not measurably catalyze the isomerization of **4** and **6**, but had the highest catalytic activity for the racemization of (+)-**7**. These results suggest that both the biphenyl moiety and the bridge moiety

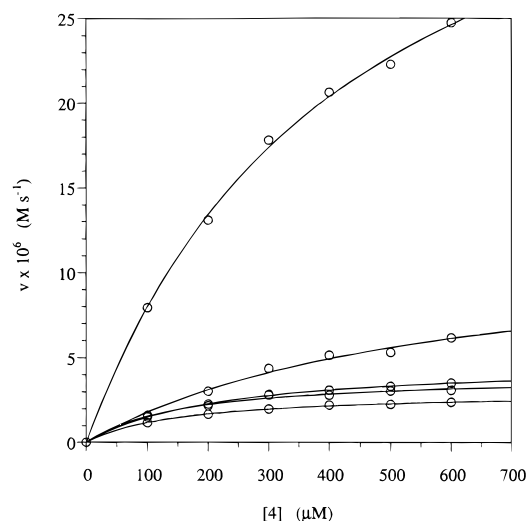


Figure 2. *V* vs [*S*] plots for the antibody-catalyzed isomerization of **4** to **6**. Data were fit to the Michaelis–Menten equation $v = V_{\max} [4]/(K_M + [4])$. The rates *v* were normalized to the protein concentration after being corrected for the background reaction. The antibodies are, from the top to the bottom, 64D8E10 (0.26 μM), 56D10D6 (1.3 μM), 51F3D2 (3.3 μM), 83F12D6 (4.2 μM), and 83F11C4 (4.9 μM).

Table 1. Kinetic Constants for the Isomerization Reaction of **4** to **6**^{a,b}

catalyst	temp (°C)	<i>K_M</i> (μM)	<i>k_{cat}</i> (s ^{−1})	<i>k_{cat}/K_M</i> (s ^{−1} M ^{−1})
mAb 51F3D2	35	250	5.2×10^{-6}	0.021
mAb 56D10D6	35	560	1.2×10^{-5}	0.021
mAb 64D8E10	35	420	4.3×10^{-5}	0.10
mAb 83F11C4	35	170	3.1×10^{-6}	0.019
mAb 83F12D6	35	190	4.1×10^{-6}	0.022
RNA AA6	28	540	4.7×10^{-7}	0.0087

^a Antibody-catalyzed reactions were carried out in 10 mM MOPS, 10 mM NaCl, pH 7.2; RNA-catalyzed reaction was carried out in 50 mM MES, 200 mM NaCl, 6 mM MgCl₂, pH 5.75. ^b $k_{\text{uncat}} = 1.5 \times 10^{-8} \text{ s}^{-1}$ at 35 °C; $k_{\text{uncat}} = 5.3 \times 10^{-9} \text{ s}^{-1}$ at 28 °C.

play an important role in the recognition of the substrates by the antibodies.

Kinetic studies initially focused on the conversion of **4** to **6**, since in this case the substrate and product are diastereomeric and can be easily separated on a reversed-phase HPLC column. Five mAbs, 51F3D2, 56D10D6, 64D8E10, 83F11C4, and 83F12D6, were chosen for further kinetic studies. Initial velocities were measured at six different concentrations of substrate **4**, ranging from 100 to 600 μM, by reversed-phase HPLC analysis. We could not use higher substrate concentrations due to poor solubility in aqueous buffer. The reaction catalyzed by each antibody was shown to obey classical Michaelis–Menten kinetics. In order to obtain kinetic constants, the data were fit directly to the Michaelis–Menten equation $v = V_{\max} [4]/(K_M + [4])$ using a nonlinear regression program (Figure 2).¹⁸ The kinetic constants at 35 °C are summarized in Table 1; the kinetic constants from the corresponding RNA-catalyzed reaction are also included.¹⁰ The *K_M* values for the antibody-catalyzed reactions are in the range of 170–560 μM, while the *k_{cat}* values are in the range of 3.1×10^{-6} to $4.3 \times 10^{-5} \text{ s}^{-1}$. The rate constant for the uncatalyzed reaction, *k_{uncat}*, under identical conditions was determined to be $1.5 \times 10^{-8} \text{ s}^{-1}$. Since the uncatalyzed reaction is a first-order reaction, one can directly compare the values of *k_{cat}* and *k_{uncat}*. The rate accelerations of the antibody-catalyzed over the uncatalyzed

(18) Siegel, I. H. *Enzyme Kinetics*; John Wiley & Sons: New York, 1975.

Table 2. Temperature Dependence of Kinetic Constants for the Isomerization of **4** to **6**

	298 K	303 K	308 K	313 K
k_{cat}^a (s^{-1})	1.18×10^{-5}	1.91×10^{-5}	4.32×10^{-5}	7.84×10^{-5}
k_{uncat} (s^{-1})	3.05×10^{-9}	7.96×10^{-9}	1.53×10^{-8}	3.37×10^{-8}

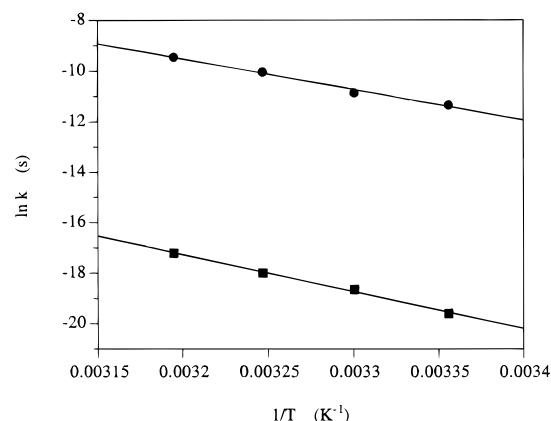
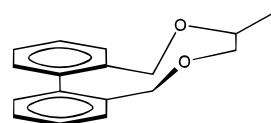
^a Catalyzed by antibody 64D8E10.

reaction ($k_{\text{cat}}/k_{\text{uncat}}$) varied from 200-fold to approximately 3000-fold. In comparison, the catalytic RNA accelerates the same reaction 88-fold over the background. Despite the rather large differences in k_{cat} values among both antibodies and RNA, all show similar K_{M} values. The difference in catalytic efficiency between antibodies and RNA is consistent with the higher binding affinities generally associated with antibodies relative to RNA aptamers.^{19,20} Indeed the K_{d} values of the antibodies range from roughly 60 to 200 nM (*vide infra*) in comparison to that of 7 μM for the catalytic RNA.

Antibody catalysis was almost completely abolished by the addition of 2 equiv of free hapten **2** to the reaction mixture, suggesting that hapten **2** is a tight binding inhibitor. However, the rate acceleration of the antibody-catalyzed reaction relative to the uncatalyzed reaction at the low concentrations of antibody required for accurate determination of K_{i} could not be measured reliably.²¹ Consequently, the K_{d} of hapten was measured by surface plasmon resonance methods.^{22,23}

The reverse reaction (**6** to **4**) catalyzed by 64D8E10 at 35 °C was also characterized. This reaction followed Michaelis–Menten kinetics with K_{M} and k_{cat} values of 580 μM and $2.4 \times 10^{-5} \text{ s}^{-1}$, respectively. The uncatalyzed reaction under the same conditions had a k_{uncat} of $5.2 \times 10^{-9} \text{ s}^{-1}$, resulting in a $k_{\text{cat}}/k_{\text{uncat}}$ of 4600. The fact that mAb 64D8E10 binds substrate **4** (S,S) slightly tighter than **6** (R,S), and catalyzes the reverse reaction with higher rate acceleration than the forward reaction likely results from the asymmetric nature of hapten **1** (dihedral angle of roughly 15°).⁷

Determination of Activation Parameters. The activation parameters (ΔH^\ddagger , ΔS^\ddagger , and ΔG^\ddagger) for the uncatalyzed reaction and the reaction catalyzed by antibody 64D8E10 were determined. The reaction rates at four different temperatures (25, 30, 35, and 40 °C) were measured (Table 2), and the activation parameters were determined from an Arrhenius plot (Figure 3).²⁴ The activation parameters for the uncatalyzed reaction are $\Delta H^\ddagger = 28.5 \text{ kcal/mol}$, $\Delta S^\ddagger = 0.43 \text{ cal/(mol}\cdot\text{K)}$, and $\Delta G^\ddagger = 28.4 \text{ kcal/mol}$. The values for the antibody-catalyzed reaction are $\Delta H^\ddagger = 23.5 \text{ kcal/mol}$, $\Delta S^\ddagger = -0.43 \text{ cal/(mol}\cdot\text{K)}$, and $\Delta G^\ddagger = 23.6 \text{ kcal/mol}$. The difference in ΔG^\ddagger between the antibody-catalyzed reaction and the uncatalyzed reaction is about 5 kcal/mol, consistent with the roughly 3000-fold rate acceleration. The ΔG^\ddagger of the uncatalyzed reaction is on the high end of activation barriers reported for similar systems.^{7,8} This may reflect increased ring strain in the transition state that results from a boatlike conformation of the bridging 10-membered ring (Figure 4). For both the catalyzed and uncatalyzed reactions, the free energy of activation (ΔG^\ddagger) is comprised largely of the enthalpy term. The reduction in ΔG^\ddagger by the antibody may be

**Figure 3.** Arrhenius plots for the antibody 64D8E10 catalyzed isomerization reaction (circles) and the uncatalyzed isomerization reaction (squares) of **4** to **6**.**Figure 4.** Putative TS[‡] for the isomerization of **4** to **6**.⁷

due to favorable binding interactions with the planar biphenyl moiety, the bridging ring system in the transition state, or both. The fact that antibody 64D8E10 did not significantly catalyze the racemization of the nine-membered ring substrate **7** supports the importance of ring strain effects in this antibody-catalyzed reaction.

Determination of Dissociation Constants. Fluorescence quenching techniques could not be used to determine the dissociation constants of the catalytic antibodies for hapten **2** since **2** did not quench antibody fluorescence.²⁵ Consequently, surface plasmon resonance assay (BIAcore analysis)^{22,23} was used to determine the dissociation constants between surface-immobilized hapten **3** and the Fab fragments of the mAbs. The surface of a sensor chip was activated with *N*-hydroxysuccinimide (NHS) and *N*-ethyl-*N'*-[3-(dimethylamino)propyl]carbodiimide hydrochloride (EDC) by standard procedures,²⁶ and hapten **3** (0.5 mM in a 10 mM MOPS, 10 mM NaCl, pH 7.2, buffer) was coupled to the surface. The unreacted NHS esters on the surface were blocked with 1.0 M ethanolamine. Negative control surfaces were generated by activating the surface with NHS and EDC, followed by blocking with 1.0 M ethanolamine.

For Scatchard analysis, injections of Fab fragments in a 10 mM MOPS, 150 mM NaCl, pH 7.2, buffer at 35 °C over hapten **3** coupled flow cell surfaces or negative control surfaces were carried out under conditions of equilibrium binding. The use of Fab fragments instead of whole antibody molecules eliminates bivalent interactions between the antibodies and the surface. Specific binding at equilibrium was obtained by subtracting the sensorgrams of the control surface from those of the hapten-coupled surface. Scatchard analysis allowed calculation of equilibrium K_{d} values (Figure 5): Fab concentrations in the range of 200–900 nM were used in the analysis. The dissociation constants obtained by this method, as well as the values of $k_{\text{cat}}/k_{\text{uncat}}$ and $K_{\text{M}}/K_{\text{d}}$, are tabulated in Table 3 (Table 3 also contains the values for the catalytic RNA).

On the basis of the notions of enzymatic TS[‡] stabilization of Pauling and Haldane,⁹ the preferential binding of the antibody to the transition state relative to the ground state should

(19) Nisonoff, A.; Hopper, J. E.; Spring, S. B. *The Antibody Molecule*; Academic Press: New York, 1975.

(20) Ellington, A. D.; Szostak, J. W. *Nature* **1990**, *346*, 818.

(21) Angeles, T. S.; Smith, R. G.; Darsley, M. J.; Sugawara, R.; Sanchez, R. I.; Kenten, J.; Schultz, P. G.; Martin, M. T. *Biochemistry* **1993**, *32*, 12128–12134.

(22) Jonsson, U.; Malmqvist, M. *Advances in Biosensors*; JAI press: London, 1992.

(23) Jonsson, U.; Fagerstam, L.; Ivarsson, B.; Johnsson, B.; Karlsson, R. *Biotechniques* **1991**, *11*, 620.

(24) Lowry, T. H.; Richardson, K. S. *Mechanism and Theory in Organic Chemistry*, 3rd ed.; Harper & Row: New York, 1987.

(25) Taira, K.; Benkovic, S. J. *J. Med. Chem.* **1988**, *31*, 129–137.

(26) *BIAapplications Handbook*; Pharmacia Biosensor AB: Uppsala, Sweden, 1994.

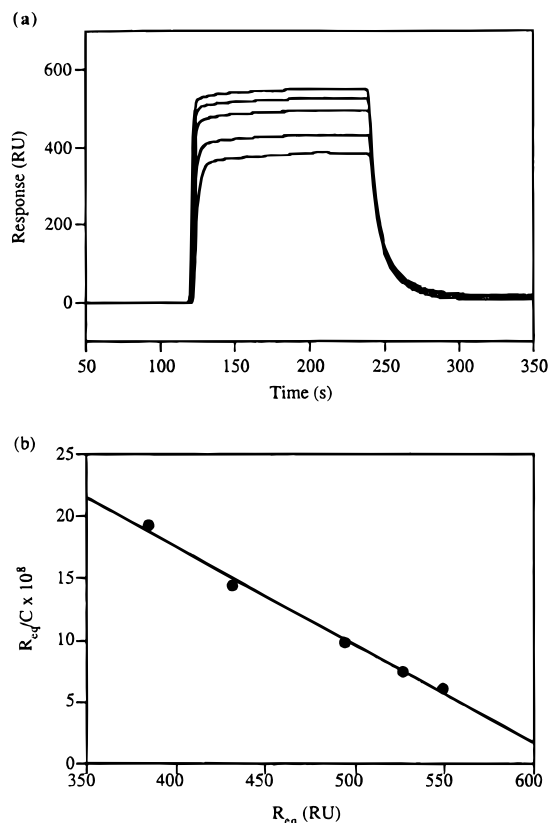


Figure 5. (a) Sensorgrams of mAb 51F3D2. (b) Scatchard plot of the data $R_{eq}/C = R_{eq}/K_d + R_{max}/K_d$, where R_{eq} is the response at equilibrium, C is the antibody concentration, and R_{max} is the maximum response.

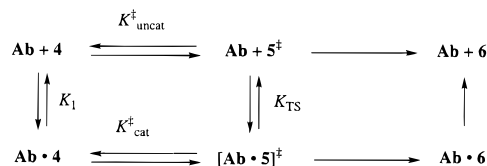
correspond to the catalytic advantage in this reaction. Accordingly, as defined in Scheme 2, $K_{cat}^{\ddagger}/K_{uncat}^{\ddagger} = K_1/K_{TS} = k_{cat}/k_{uncat}$, where K_{cat}^{\ddagger} is an equilibrium constant between $Ab \cdot 4$ and $[Ab \cdot 5]^{\ddagger}$, K_{uncat}^{\ddagger} is an equilibrium constant between 4 and 5^{\ddagger} , K_1 is a dissociation constant between antibody and 4 , and K_{TS} is a dissociation constant between antibody and 5^{\ddagger} . K_1 can be substituted by K_M , and K_{TS} can be substituted by K_d (the dissociation constant for antibody and hapten) when the hapten is a good transition state analogue. Thus, one can obtain the relationship of $K_M/K_d = k_{cat}/k_{uncat}$. In the case of the fastest antibody, 64D8E10, as well as the RNA, these two values agree well and the binding energy correlates with the rate enhancement. However, there is not a good correlation in the other antibody-catalyzed reactions. The values of K_M/K_d range from 2000 to 3000 for all the antibodies, corresponding to $\Delta\Delta G^{\ddagger}$ values of 4.5–4.8 kcal/mol, whereas the values of k_{cat}/k_{uncat} range from 200 to 2700.

Table 3. A Comparison of $K_M(4)$, $K_d(3)$, $K_M(4)/K_d(3)$, and k_{cat}/k_{uncat} Values for the Isomerization of **4** to **6**

catalyst	$K_M(4)$ (μ M)	$K_d(3)$ (nM)	$K_M(4)/K_d(3)$	k_{cat}/k_{uncat}
mAb 51F3D2	250	130	2000	340
mAb 56D10D6	560	180	3100	770
mAb 64D8E10	420	210	2000	2900
mAb 83F11C4	170	60	2700	200
mAb 83F12D6	190	70	2800	270
RNA AA6	540	7000 ^a	77	88

^a Determined by inhibition kinetics using compound **2** as an inhibitor.

Scheme 2



These results indicate that binding energy is being used nonproductively for the majority of antibodies, and/or that hapten **3** is not an ideal TS^{\ddagger} analogue for the isomerization of substrate **4** to product **6**. This may result from unfavorable interactions between the antibodies and the bridging ring in the substrate molecule which is not well mimicked by the hapten. At the same time, the reaction is more complex than rotation around a single carbon–carbon σ bond; rotations around the other σ bonds in the 10-membered ring bridge are required and likely contribute significantly to the free energy of activation of the reaction. The antibodies may all stabilize the planar conformation of the biphenyl in the transition state but may vary in their ability to stabilize a high-energy conformation of the bridging ring system (recall that the bridge is near the conjugation site in the hapten which may lead to decreased binding by antibodies).¹⁹ The differences in the catalytic activities of the antibodies toward the 9- and 10-membered ring substrates support the importance of ring strain in catalysis. Nevertheless, even for the slowest antibody, 83F11C4, approximately 70% of the binding energy is translated into catalysis.

Acknowledgment. We are grateful for financial support for this work from the National Institutes of Health (Grant No. R01AI24695). P.G.S. is a Howard Hughes Medical Institute Investigator. T.U. was supported by a fellowship from Berlex Biosciences, and J.K. and J.R.P. were supported by NIH Biotechnology Training Grant (GM08352A). We thank E. Sweet and Y. Oei for assistance with antibody production.

JA9542449